Science Bulletin 64 (2019) 380–384

Contents lists available at ScienceDirect

Science Bulletin

journal homepage: www.elsevier.com/locate/scib

Article

Nonadiabatic dynamics and geometric phase of an ultrafast rotating electron spin

Xing-Yan Chen [a,b,c], Tongcang Li [d,e,f,g], Zhang-Qi Yin [a,*]

[a] Center for Quantum Information, Institute for Interdisciplinary Information Sciences, Tsinghua University, Beijing 100084, China
[b] Max-Planck-Institut für Quantenoptik, Garching 85748, Germany
[c] Fakultät für Physik, Ludwig-Maximilians-Universität München, München 80799, Germany
[d] Department of Physics and Astronomy, Purdue University, West Lafayette, Indiana 47907, USA
[e] School of Electrical and Computer Engineering, Purdue University, West Lafayette, Indiana 47907, USA
[f] Purdue Quantum Center, Purdue University, West Lafayette, Indiana 47907, USA
[g] Birck Nanotechnology Center, Purdue University, West Lafayette, Indiana 47907, USA

ARTICLE INFO

Article history:
Received 29 November 2018
Received in revised form 22 January 2019
Accepted 14 February 2019
Available online 26 February 2019

Keywords:
Nitrogen-vacancy center
Nonadiabatic geometric phase
Ultrafast rotor
Rabi oscillation
Optomechanics

ABSTRACT

The spin in a rotating frame has attracted a lot of attentions recently, as it deeply relates to both fundamental physics such as pseudo-magnetic field and geometric phase, and applications such as gyroscopic sensors. However, previous studies only focused on adiabatic limit, where the rotating frequency is much smaller than the spin frequency. Here we propose to use a levitated nano-diamond with a built-in nitrogen-vacancy (NV) center to study the dynamics and the geometric phase of a rotating electron spin without adiabatic approximation. We find that the transition between the spin levels appears when the rotating frequency is comparable to the spin frequency at zero magnetic field. Then we use Floquet theory to numerically solve the spin energy spectrum, study the spin dynamics and calculate the geometric phase under a finite magnetic field, where the rotating frequency to induce resonant transition could be greatly reduced.

1. Introduction

The electron and nuclear spins in a rotating frame are deeply connected to both fundamental physics and applications. The frequencies of the spins will shift in the rotating frame, which can be explained by an emerged pseudo-magnetic field [1,2]. The quantum mechanical geometric phase was also predicted to appear in these systems in adiabatic limit, where the frequency of rotating frame is much less than the frequencies of the spins [3–5]. The pseudo-magnetic field has been detected by both nuclear [6] and electron spins [7,8]. However, the corresponding geometric phase which is proportional to the rotating frequency and can be used as a gyroscopic sensor [9], has been too small to be measured in a traditional mechanical rotor with a maximum rotation frequency of about 10 kHz [8].

Here we propose to use a levitated nanodiamond that can be driven to rotate at an ultrahigh speed in vacuum to study the geometric phase of a rotating electron spin. Our proposal is based on recent breakthroughs in levitated optomechanics [10–24]. Nanodiamonds with nitrogen-vacancy centers that host electron spins have been levitated in vacuum with optical tweezers [25–27], ion traps [28,29], and magneto-gravitational traps [30]. Recently, rotation frequencies larger than 1 GHz have been experimentally observed with optically levitated nanoparticles driven by circularly-polarized lasers [31,32]. In this way, for the first time, the frequency of a mechanical rotor approaches the frequency of the electron spin in the NV center and previous studies based on adiabatic approximation will no longer be valid [3–5]. A theory of nonadiabatic spin dynamics and geometric phase in a rotating frame is needed.

In this paper, we study the electron spin dynamics and calculate the quantum geometric phase of an NV center in an ultra-fast rotating levitated nanodiamond without adiabatic approximation. The Hamiltonian we obtained is similar to a spin-1 molecule in an external magnetic field [33]. However, in our case the origin of the geometric phases is purely mechanical. Furthermore, by using the Floquet analysis, our discussion is not limited to adiabatic limit which is the case for most of the previous studies in such systems. In the nonadiabitc regime, Rabi oscillations between the spin states appear when the angle θ between the axis of the NV center and the axis of the rotor is not zero. A selection rule for

* Corresponding author.
E-mail address: yinzhangqi@mail.tsinghua.edu.cn (Z.-Q. Yin).

https://doi.org/10.1016/j.scib.2019.02.018
2095-9273/

different spin states naturally appears, in accordance with the angular momentum conservation. Though these Rabi oscillations are obtained without any external field, we find that the resonant transitions could be achieved with much lower rotating frequency with an external magnetic field.

2. The model

We consider a non-spherical nano-diamond optically trapped in high vacuum. The length of the three axes of the nanodiamond are different. Therefore, its rotational degrees of freedom could be manipulated by the driving laser. We adopt the polarization of the driving laser to be circular. The nano-diamond could be driven to rotate at a constant angular velocity ω [31,32]. There is a nitrogen-vacancy center, with electron spin $S=1$, in the nanodiamond. As shown in Fig. 1a, we choose the direction of $\boldsymbol{\omega}$ along z-axis, and define spherical coordinates θ and ϕ. We denote θ as the angle between the rotational axis and the axis of the NV center, and $\phi(t)=\omega t$. For simplicity, we consider the dynamics of the electron spin without external magnetic field at first. The Hamiltonian of the rotating NV center can be obtained by a rotational transformation $R(t)=R_z(\phi(t))R_y(\theta)$ on the stationary Hamiltonian $H_0=DS_z^2$ ($\hbar=1$), which reads $H(t)=R(t)H_0R^\dagger(t)$. Here the rotation of spin-1 by the angle α along direction $\mathbf{n}$ is given by $R(\alpha)=\mathrm{e}^{-\mathrm{i}\alpha\mathbf{n}\cdot\mathbf{S}}$.

The Hamiltonian $H(t)$ is written in the spin basis in the inertial (lab) frame. Alternatively, we can rewrite the Hamiltonian in the basis which rotate with the solid spin and study the dynamics of a rotating spin. The unitary transformation from the static basis to the rotating basis is given by $W^\dagger(t)=R(t)R_z(-\phi(t))$, which differs from $R(t)$ by an additional $R_z(-\phi(t))$ rotation. The rotational transformation corresponding to $R(t)$ and $W(t)$ are shown in Fig. 1b, which are denoted by $Ox'y'z'$ and $Ox''y''z''$, respectively. The additional term $R_z(-\phi(t))$, which cancels the rotation of the local orthogonal coordinates, moves the geometric phase into the dynamical phase [34]. To see that, we write down the Hamiltonian after the unitary transform

$$\begin{aligned}\widetilde{H}(t)&=W(t)H(t)W^\dagger(t)+\mathrm{i}\partial_tW(t)W^\dagger(t)\\&=H_0+\omega(1-\cos\theta)S_z+\tfrac{\omega}{2}\sin\theta\left[\mathrm{e}^{-\mathrm{i}(\omega t+\phi_0)}S_++h.c.\right],\end{aligned}\tag{1}$$

where $S_\pm=S_x\pm\mathrm{i}S_y$. The constant phase ϕ_0 in Eq. (1) arises when $Ox'y'z'$ and $Ox''y''z''$ in Fig. 1b have a relative rotation $R_z(-\phi_0)$.

In the interaction picture given by the unitary transformation $U=\mathrm{e}^{\mathrm{i}\omega S_zt}$, the time-independent Hamiltonian reads

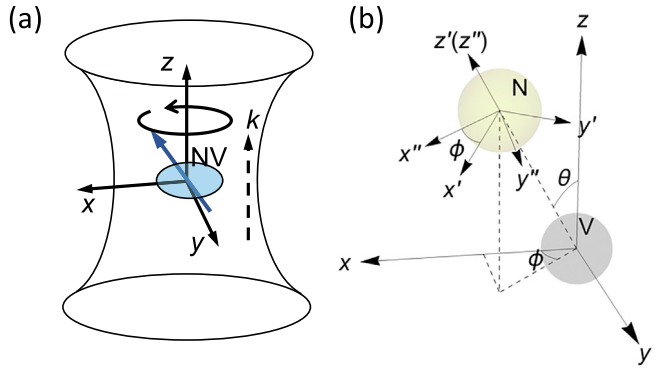

Fig. 1. (Color online) The schematic of the model. (a) A nanodiamond with a build-in NV center is levitated in an optical trap. A circularly polarized laser drives the nanodiamond to rotate at angular frequency ω. (b) The frames $Ox'y'z'$ and $Ox''y''z''$ are defined by the rotational transformations $R(t)=R_z(\phi(t))R_y(\theta)$ and $W^\dagger(t)=R(t)R_z(-\phi(t))$, respectively. The rotating spin states are defined to be static in the frame $Ox''y''z''$.

$$\widetilde{H}_I=\begin{pmatrix}D-\omega\cos\theta & \Omega^*/2 & 0\\ \Omega/2 & 0 & \Omega^*/2\\ 0 & \Omega/2 & D+\omega\cos\theta\end{pmatrix},\tag{2}$$

where we denote $\Omega=\sqrt{2}\omega\mathrm{e}^{\mathrm{i}\phi_0}\sin\theta$ as the Rabi frequency. In the rest of this paper, the phase ϕ_0 of the Rabi frequency is eliminated by redefining the S_z states.

Let us solve the Hamiltonian (2) at two limits at first, the adiabatic limit $\omega\ll D$ and the near resonant limit $|D\pm\omega\cos\theta|\ll\Omega$. In the adiabatic limit, the effect of transitions between spin states is negligible. We can neglect the off-diagonal terms in Hamiltonian (1) and get the effective Hamiltonian $\widetilde{H}_e=DS_z^2+\omega(1-\cos\theta)S_z$, where the last term $\omega(1-\cos\theta)S_z$ is called the rotating induced level shift (RILS) term [3–5]. When $|D\pm\omega\cos\theta|<\Omega$, the off-diagonal terms in the Hamiltonian (2) could induce transitions between $|0\rangle$ and $|\pm1\rangle$. The resonant condition requires the angular frequency $\omega_\pm=\pm D/\cos\theta$. At resonance, and in the limit $\sin\theta\ll1$, we can ignore off-resonant terms and get Rabi oscillation in a two-dimensional subspace with the Rabi frequency $|\Omega|$. For rotating frequency $\omega=\omega_+$, the resonant transition between $|0\rangle$ and $|+1\rangle$ happens, while for $\omega=\omega_-$ the resonant transition between $|0\rangle$ and $|-1\rangle$ appears. This driving selectivity comes from the conservation of angular momentum.

For an arbitrary ω and θ, the whole 3×3 matrix of the Hamiltonian (2) needs to be diagonalized. The quasi-energies are given by the solution of the cubic equation

$$\lambda^3-2D\lambda^2-\left(\omega^2-D^2\right)\lambda+\omega^2D\sin^2\theta=0,\tag{3}$$

which are λ_0 and $\lambda_{\pm1}$. We denote the Floquet states with quasi-energies λ_n by $|\lambda_n\rangle$, with $n=0,\pm1$. Here, $|\lambda_n\rangle$ smoothly connects to $|n\rangle$ at the adiabatic limit $\omega\ll D$. The quasi-energy spectrum as a function of ω and θ is shown in Fig. 2a. The quasi-energy spectrum λ has a level crossing around $\omega=\pm D$ if $\theta=0$. As long as $\theta\neq0$, the quasi-energy spectrum has an avoided level crossing near the resonant point $\omega_\pm$, as shown in Fig. 2b. The quasi-energy splitting at the resonant point gives the Rabi frequency Ω. In Fig. 2a, there is also an avoided level crossing between $|+1\rangle$ and $|-1\rangle$ near $\theta=\pi/2$, which corresponds to Rabi oscillation between these two states with Rabi frequency ω^2/D. This oscillation can be explained by calculating the second order effective Hamiltonian as discussed in Supplementary data. We plot the dynamics of the electron spin in an NV center in the rotating frame in Supplementary data.

If the NV center is rotating in the presence of an non-zero external magnetic field, as shown in Supplementary data, the total Hamiltonian reads $H(t)=R(t)\left(DS_z^2+g\mu_\mathrm{B}B\mathbf{S}\cdot\mathbf{n}\right)R^\dagger(t)=R(t)H_1R^\dagger(t)$, where $\mathbf{n}=(\sin\theta,\cos\theta,0)$ is the unitary vector along the magnetic field direction in the rotating frame, and $\Delta=-g\mu_\mathrm{B}B$. Similar to Eq. (1), we apply the unitary transformation $\widetilde{H}_1(t)=W(t)H_1(t)W^\dagger(t)+i\partial_tW(t)W^\dagger(t)$ and get

$$\begin{aligned}\widetilde{H}(t)=DS_z^2-\Delta\cos\theta S_z+\Delta\sin\theta S_x+\omega(1-\cos\theta)S_z+\frac{\omega}{2}\\\times\sin\theta\left(\mathrm{e}^{-\mathrm{i}\omega t}S_++h.c.\right).\end{aligned}\tag{4}$$

The presence of the magnetic field change the eigenstates of the spin, which are no longer the eigenstates of operator S_z. When the spin is rotating, the time-independent eigenstates will be further changed. Therefore, it is quite difficult to analytically solve the problem. However, in the limit of $\theta\ll1$, the magnetic field does not change the eigenstates to the first order of θ. Therefore, for simplicity, we consider $0<\Delta<D$ with the small angle limits $\theta\ll1-\Delta/D$, and only consider the nearly resonant situation. The effective Hamiltonian (to the order of θ^2) is derived in Supplementary data, the result is

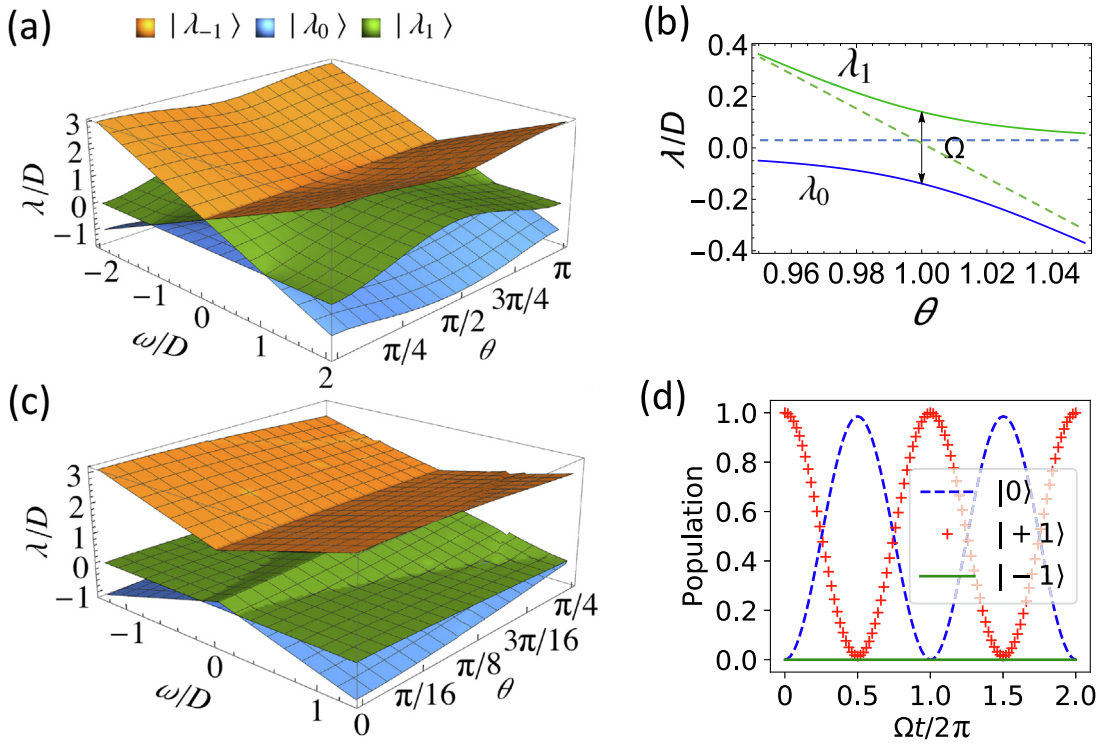

Fig. 2. (Color online) The quasi-energies and the spin dynmics. (a) The quasi-energies $\lambda_{0,\pm}$ as a function of rotating frequency ω and θ. When near crossover $\omega = \pm D/\cos\theta$, the eigenstates of S_z will be significantly mixed, which means that there will be Rabi oscillation. The index $n = 0, +1, -1$ means that at $\omega = 0$ the Floquet states reduce to $|S_z = n\rangle$. (b) is the scaled slice with $\theta = \pi/100$ in (a). The quasi-energy splitting gives the Rabi frequency Ω. (c) and (d) are the numerical solution of quasi-energies and time-evolution in the presence of a static magnetic field with $\Delta = 0.803D$. The magnetic field satisfies the resonant condition with $\theta = \pi/100$ and $\omega = 0.2D$ in (d). The quasi-energies are obtained by diagonalizing the Floquet Hamiltonian.

$$\widetilde{H}(t) = \widetilde{D}S_z^2 - \tilde{\Delta}S_z + \frac{\omega}{2}\theta\left(e^{-i\omega t}S_+ + h.c.\right), \tag{5}$$

where $\widetilde{D} = D + \frac{3D\Delta^2}{2(D^2-\Delta^2)}\theta^2$ and $\tilde{\Delta} = \Delta - \frac{1}{2}\omega\theta^2 - \frac{D^2\Delta}{2(D^2-\Delta^2)}\theta^2$. The resonant condition is given by $\widetilde{D} \mp \tilde{\Delta} = \pm\omega$. Therefore, the magnetic field compensate to ω and allows us to observe Rabi oscillation at a lower angular frequency.

When the angle θ is not approaching zero, the above perturbative analysis becomes invalid, and we adopt the Floquet formalism [35,36] to numerically solve the evolution of Eq. (4), as shown in Supplementary data. Since the quasi-energies are determined uniquely only up to a multiple of ω, the branches start at the same quasi-energy with slopes $+n\omega$ and represent the same Floquet states with quasi-energy $+n\omega$. For example, an avoided level crossing between $|\lambda_0\rangle$ start with slope 0 and $|\lambda_{+1}\rangle$ start with slope $-\omega$ means there is strong transition from $|0\rangle$ to $|+1\rangle$ by absorbing one photon. In order to compare with quasi-energies under the zero magnetic field, as shown in Fig. 2, we choose the three quasi-energy branches that smoothly connected to the $\omega = 0$ eigenvalues with slopes equal to $\omega, 0$, and $-\omega$ for $|\lambda_{-1}\rangle, |\lambda_0\rangle$, and $|\lambda_{+1}\rangle$, respectively.

We numerically solve the quasi-energies with external magnetic field. As shown in Fig. 2c, there is an avoided level crossing between $|\lambda_0\rangle$ and $|\lambda_{+1}\rangle$ for $\theta \neq 0$. The resonant angular frequency ω increases if the angle between the spin and the rotating axis θ increases. The quasi-energy splitting corresponds to the Rabi frequency $\Omega = \sqrt{2}\omega\sin\theta$. If there is no magnetic field, for $\theta = \pi/100$ and $\omega = 0.2D$, the Rabi oscillation between $|0\rangle$ and $|+1\rangle$ is negligible. By applying a static magnetic field with $\Delta = 0.803D$ to meet the resonant condition, as shown in Fig. 2d, there is a resonant Rabi oscillation between $|0\rangle$ and $|+1\rangle$. In this way, the resonant electron spin dynamics could be realized with rotating frame frequency ω much lower than D.

3. Non-adiabatic geometric phase

Based on the Floquet formalism, as shown in Supplementary data, we can derive the non-adiabatic geometric phase for the electron spin of the NV center in an ultra-fast rotating nanodiamond. The non-adiabatic geometric phases for the cyclic states are defined as [37–39],

$$\gamma_n = i\int_0^T \left\langle \lambda_n(t)|\frac{d}{dt}|\lambda_n(t)\right\rangle dt - \delta_n, \tag{6}$$

where $|\lambda_n\rangle$ is the Floquet state and δ_n denotes the dynamical phase. Let us consider the case without external magnetic field first. In Supplementary data, we show that the Eq. (6) can be rewritten as $\gamma_n = \int_0^T \left\langle \lambda_n|\widetilde{H}_I - DS_z^2 + \omega S_z|\lambda_n\right\rangle dt$, and plug in the coefficient of Floquet states, we get

$$\gamma_n = \frac{2\pi}{\omega}\left(\lambda_n - (D-\omega)|c_{n,+1}|^2 - (D+\omega)|c_{n,-1}|^2\right), \tag{7}$$

where $c_{n,k}, k = 0, \pm1$ are the coefficients of $|\lambda_n\rangle$ in the spin basis, i.e., $|\lambda_n\rangle = \sum_{k=0,\pm1} c_{n,k}|S_z = k\rangle$. Based on the simplified Hamiltonian in the limit $\omega \ll D$ and $\omega \sim D/\cos\theta$, we can obtain the geometric phase using Eq. (7). If the rotation is adiabatic $\omega \ll D$, the Floquet states $|\lambda_n\rangle$ has almost no mixing between the spin states. The quasi-energies $\lambda_{+1}, \lambda_0, \lambda_{-1} = D + \omega\cos\theta, 0, D - \omega\cos\theta$, with corresponding geometric phases $\gamma_{+1}, \gamma_0, \gamma_{-1} = 2\pi(1-\cos\theta), 0, -2\pi(1-\cos\theta)$, which are consistent with the previous studies [3–5]. Near resonance where $\omega \simeq D/\cos\theta$ and $\theta \ll 1$, there is strong mixing between spin states. The corresponding Floquet states are $|\lambda_{+1}\rangle = (|0\rangle + |+1\rangle)\sqrt{2}, |\lambda_0\rangle = (|0\rangle - |+1\rangle)\sqrt{2}$, and $|\lambda_{-1}\rangle = |-1\rangle$ with quasi-energies $\lambda_{+1}, \lambda_0, \lambda_{-1} = \Omega/2, -\Omega/2, 2D$. The non-adiabatic geometric phases are $\gamma_{+1}, \gamma_0, \gamma_{-1} = \sqrt{2}\pi\sin\theta, -\sqrt{2}\pi\sin\theta, 0$. As

shown in Fig. 3a, a slightly detuning from resonance will reduce the geometric phase, which means that for small angles θ the geometric phase will maximize at resonance. For general situations with arbitrary ω and θ, we provide numerical results in Fig. 3b. The analysis for limit cases indicates that there is crossing between the two limits. Also, the peak behavior at resonance $\omega = D/\cos\theta$ is demonstrated. When θ increases, the geometric phases become larger, but the peak is not so apparent due to the break down of two-level approximation at the large angle. From Fig. 3b, the crossing at $\theta = \pi/2$ corresponds to the second order Rabi oscillation between $|\pm 1\rangle$, and the crossing at $\theta \sim \pi$ and $\omega \simeq D$ corresponds to the Rabi oscillation similar to the small angle.

From Eq. (7) we can also reveal the relation between quasi-energy λ_n and geometric phase γ_n. In adiabatic limit, the geometric phase is identical to the phase of RILS term accumulating in a single period. At the resonance point, the geometric phases for the two resonant states are given by their Rabi frequency accumulate in a single period. In this two situations, the measurement of the geometric phase and the quasi-energy are equivalent.

The adiabatic geometric can be used for measuring rotating frequency in the adiabatic limit [3–5,7,8]. Our analysis shows that this method still works in the nonadiabatic regime $\omega \sim D$, where the nonadiabatic geometric phase can be measured with spectroscopic or interference [40–42]. Moreover, as the rotating frequency can be determined with high precision by measuring the scattering photon of the nano-diamond [31,32], the angle θ could be measured through the Floquet quasi-energy spectrum [43–45]. In the limit $\theta \ll 1$, the measurement of quasi-energies is equivalent to the measuerement of the Rabi frequency Ω. The uncertainty of the angular measurement $\delta\theta = \delta\Omega/\left(\sqrt{2}\omega\cos\theta\right)$ is inversely proportional to rotating frequency ω and minimized around $\theta = 0$.

Under external magnetic field, Eq. (6) for the non-adiabatic geometric phases still applies, except that the Floquet states are different from those without external field. For simplicity, we only analyze the limit case where $\omega \sim 0$ and near resonance, and for small angle θ where the Hamiltonian is given by Eq. (5). From Eq. (6), when apply to $\omega \sim 0$ case the geometric phases are $2\pi(1-\cos\theta)S_z$ which are the same as zero field. This is because the magnetic field only shifts the energy level therefore only affects the dynamical phases. At resonance, the geometric phases for the two resonant states are proportional to the Rabi frequency, given by $\pm\sqrt{2}\pi\sin\theta$ which are also the same as zero field.

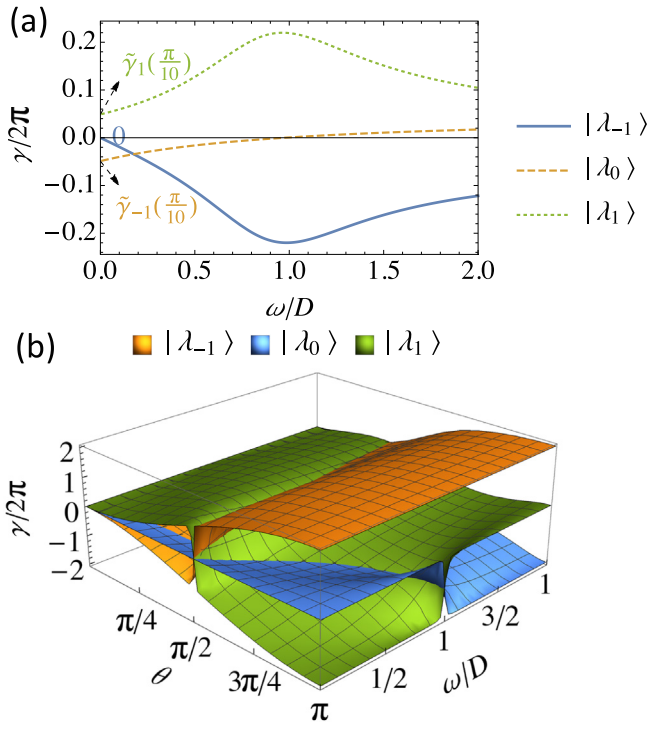

Fig. 3. (Color online) The non-adiabatic geometric phases $\gamma_{0,\pm}$. (a) Relation between the $\gamma_{0,\pm}$ and rotating frequency ω for the three cyclic states $\lambda_{0,\pm}$ under the angle $\theta = \pi/10$. At adiabatic limit $\omega \ll D$, the geometric phases are given by $\tilde{\gamma}_{\pm1}(\theta) = \pm 2\pi(1-\cos\theta)$. At resonance point $\omega = D/\cos\theta$, the geometric phases are $\gamma_{+1}, \gamma_0, \gamma_{-1} = \sqrt{2}\pi\sin\theta, -\sqrt{2}\pi\sin\theta, 0$. (b) Non-adiabatic geometric phases $\gamma_{0,\pm}$ for the three cyclic states under different rotating frequency ω and angle θ.

4. Discussion and conclusion

We briefly discuss the experimental feasibility. As the silica-based nano-particles have been driven to the GHz rotating frequency regime, we believe that it is also possible to optically drive the nanodiamond to rotate in GHz. The main obstacle is the optical heating of the NV center in diamond, which could be resolved by adopting pure diamond [46] and using nano-refrigerator [47]. The Rabi frequency induced by the GHz rotation is usually in the order of 1–100 MHz, which is much larger than the dephasing rate of the NV center in a nanodiamond [48]. In the rotating nanodiamond, the NV center could be decoupled from the nuclear spin bath and has longer dephasing time than in the static frame [49]. Therefore, the dephasing effect of the NV center will not prevent the observation of these efforts.

Previous experiments have demonstrated initialization and readout of a rotating NV spin [8,49,50]. In our case, following the spinning nanodiamond, the position of a NV center rotates within a radius less than 100 nm, which is much less than the wavelength of the zero phonon emission of the NV center. So the position of the NV center will be maintained within the focus of the detection system. The standard initialization and readout method for the NV center could be applied to measure the shifts of energy levels, observe Rabi oscillation and measure geometric phases. The measurement speed can be slower than the rotating speed because the Rabi oscillation frequency is much smaller than the rotation frequency of the NV center.

In conclusion, we study the electrons spin dynamics and geometric phase in a levitated ultra-fast rotating nanodiamond, without adiabatic approximation. The Rabi oscillation appears if the rotating frequency matches the electron spin levels splitting, even without an external magnetic field. The nonadiabatic geometric phase of the electron spin induced by ultra-fast rotation is explored and could be used to build an angular sensor. The proper external magnetic field would greatly decrease the rotating frequency for resonantly transition and makes it easier for experimental realization. Similar phenomena may also appear in the nuclear spins in a rotating frame, with much lower rotating frequency. As recently being demonstrated in experiment [51], the rotation of the nanodiamond could also evolve precession and nutation. Our next step is to describe the spin dynamics in such general rotating frame. Another interesting topics is to explore the relativistic quantum phenomena in the ultra-faster rotating frame.

Conflict of interest

The authors declare that they have no conflict of interest.

Acknowledgments

Z.Q.Y. is supported by the National Natural Science Foundation of China (61771278 and 61435007), and the Joint Foundation of Ministry of Education of China (6141A02011604). T.L. is supported by NSF under Grant No. PHY-1555035. We thank the helpful discussions with Nan Zhao and Ying Li.

Author contributions

Z.Q.Y. and T.L. designed the study. X.C. performed the analysis under the supervision of Z.Q.Y. T.L. provided the support on experimental feasibility. All authors contributed to writing the manuscript.

Appendix A. Supplementary data

Supplementary data associated with this article can be found, in the online version, at https://doi.org/10.1016/j.scib.2019.02.018.

References

[1] Barnett SJ. Magnetization by rotation. Phys Rev 1915;6:239.
[2] Barnett SJ. Gyromagnetic and electron-inertia effects. Rev Mod Phys 1935;7:129.
[3] Ajoy A, Cappellaro P. Stable three-axis nuclear-spin gyroscope in diamond. Phys Rev A 2012;86:062104.
[4] MacLaurin D, Doherty MW, Hollenberg LCL, et al. Measurable quantum geometric phase from a rotating single spin. Phys Rev Lett 2012;108:240403.
[5] Ledbetter MP, Jensen K, Fischer R, et al. Gyroscopes based on nitrogen-vacancy centers in diamond. Phys Rev A 2012;86:052116.
[6] Chudo H, Ono M, Harii K, et al. Observation of Barnett fields in solids by nuclear magnetic resonance. Appl Phys Express 2014;7:063004.
[7] Wood AA, Lilette E, Fein YY, et al. Magnetic pseudofields in a rotating electron-nuclear spin system. Nat Phys 2017;13:1070.
[8] Wood AA, Lilette E, Fein YY, et al. Quantum measuremen of a rapidly rotating spin qubit in diamond. Sci Adv 2018;4:eaar7691.
[9] Zhang C, Yuan H, Tang Z, et al. Inertial rotation measurement with atomic spins: from angular momentum conservation to quantum phase theory. Appl Phys Rev 2016;3:041305.
[10] Yin ZQ, Geraci AA, Li T. Optomechanics of levitated dielectric particles. Int J Mod Phys B 2013;27:1330018.
[11] Chang DE, Regal CA, Papp SB, et al. Cavity optomechanics using an optically levitated nanosphere. Proc Natl Acad Sci USA 2010;107:1005.
[12] Romero-Isart O, Juan ML, Quidant R, et al. Toward quantum superposition of living organisms. New J Phys 2010;12:033015.
[13] Yin ZQ, Li TC, Zhang X, et al. Large quantum superpositions of a levitated nanodiamond through spinoptomechanical coupling. Phys Rev A 2013;88:033614.
[14] Scala M, Kim MS, Morley GW, et al. Matter wave interferometry of a levitated thermal nano-oscillator induced and probed by a spin. Phys Rev Lett 2013;111:180403.
[15] Shi H, Bhattacharya M. Optomechanics based on angular momentum exchange between light and matter. J Phys B 2016;49:153001.
[16] Hoang TM, Ma Y, Ahn J, et al. Torsional optomechanics of a levitated nonspherical nanoparticle. Phys Rev Lett 2016;117:123604.
[17] Ma Y, Hoang TM, Gong M, et al. Proposal for quantum many-body simulation and torsional matter-wave interferometry with a levitated nanodiamond. Phys Rev A 2017;96:023827.
[18] Arita Y, Mazilu M, Dholakia K. Laser-induced rotation and cooling of a trapped microgyroscope in vacuum. Nat Commun 2013;4:2374.
[19] Kuhn S, Stickler BA, Kosloff A, et al. Optically driven ultra-stable nanomechanical rotor. Nat Commun 2017;8:1670.
[20] Monteiro F, Ghosh S, van Assendelft EC, et al. Optical rotation of levitated spheres in high vacuum. Phys Rev A 2018;97:051802.
[21] Stickler BA, Schrinski B, Hornberger K. Rotational friction and diffusion of quantum rotors. Phys Rev Lett 2018;121:040401.
[22] Zhao N, Yin ZQ. Room-temperature ultrasensitive mass spectrometer via dynamical decoupling. Phys Rev A 2014;90:042118.
[23] Ranjit G, Cunningham M, Casey K, et al. Zeptonewton force sensing with nanospheres in an optical lattice. Phys Rev A 2016;93:053801.
[24] Monteiro F, Ghosh S, Fine AG, et al. Optical levitation of 10-ng spheres with nano-g acceleration sensitivity. Phys Rev A 2017;96:063841.
[25] Yin Z, Zhao N, Li T. Hybrid opto-mechanical systems with nitrogen-vacancy centers. Sci China Phys Mech Astron 2015;58:050303.
[26] Neukirch LP, von Haartman E, Rosenholm JM, et al. Multi-dimensional single-spin nano-optomechanics with a levitated nanodiamond. Nat Photonics 2015;9:653.
[27] Hoang TM, Ahn J, Bang J, et al. Electron spin control of optically levitated nanodiamonds in vacuum. Nat Commun 2016;7:12250.
[28] Conangla GP, Schell AW, Rica RA, et al. Motion control and optical interrogation of a levitating single nitrogen vacancy in vacuum. Nano Lett 2018;18:3956.
[29] Delord T, Huillery P, Schwab L, et al. Ramsey interferences and spin echoes from electron spins inside a levitating macroscopic particle. Phys Rev Lett 2018;121:053602.
[30] Hsu JF, Ji P, Lewandowski C, et al. Cooling the motion of diamond nanocrystals in a magneto-gravitational trap in high vacuum. Sci Rep 2016;6:30125.
[31] Ahn J, Xu ZJ, Bang J, et al. Optically levitated nanodumbbell torsion balance and GHz nanomechanical rotor. Phys Rev Lett 2018;121:033603.
[32] Reimann R, Doderer M, Hebestreit E, et al. GHz rotation of an optically trapped nanoparticle in vacuum. Phys Rev Lett 2018;121:033602.
[33] Meyer E, Leanhardt AE, Cornell EA. Berrylike phases in structured atoms and molecules. Phys Rev A 2009;80:062110.
[34] Giavarini G, Gozzi E, Rohrlich D, et al. On removing Berry's phase. Phys Lett A 1989;138:235–41.
[35] Grifoni M, Hänggi P. Driven quantum tunneling. Phys Rep 1998;304:229.
[36] Shirley JH. Solution of the schrödinger equation with a hamiltonian periodic in time. Phys Rev 1965;138:B979.
[37] Aharonov Y, Anandan J. Phase change during a cyclic quantum evolution. Phys Rev Lett 1987;58:1593.
[38] Moore DJ, Stedman GE. Non-adiabatic Berry phase for periodic Hamiltonians. J Phys A Math Gen 1990;23:2049.
[39] Moore DJ. Floquet theory and the non-adiabatic Berry phase. J Phys A Math Gen 1990;23:L665.
[40] Anandan J. The geometric phase. Nature 1992;360:307.
[41] Appelt S, Wäckerle G, Mehring M. A magnetic resonance study of non-adiabatic evolution of spin quantum states. Z Phys D 1995;34:75.
[42] Das R, Kumar SKK, Kumar A. Use of non-adiabatic geometric phase for quantum computing by NMR. J Magn Reson 2005;177:318.
[43] Iliescu D, Fishman S, Ben-Jacob E. Quasienergy spectroscopy in mesoscopic systems. Phys Rev B 1992;46:14675.
[44] Tuorila J, Silveri M, Sillanpää M, et al. Stark effect and generalized bloch-siegert shift in a strongly driven twolevel system. Phys Rev Lett 2010;105:257003.
[45] Shu Z, Liu Y, Cao Q, et al. Observation of floquet Raman transition in a driven solid-state spin system. Phys Rev Lett 2018;121:210501.
[46] Gines L, Frangeskou AC, Rahman ATMA, et al. Optical levitation of high purity nanodiamonds in vacuum without heating. New J Phys 2018;20:043016.
[47] Rahman ATMA, Barker PF. Laser refrigeration, alignment and rotation of levitated Yb^{3+}:YLF nanocrystals. Nat Photonics 2017;11:634.
[48] Knowles HS, Kara DM, Atatüre M. Observing bulk diamond spin coherence in high-purity nanodiamonds. Nat Mater 2014;13:21.
[49] Wood AA, Aeppli AG, Lilette E, et al. T_2-limited sensing of static magnetic fields via fast rotation of quantum spins. Phys Rev B 2018;98:174114.
[50] Kowarsky MA, Hollenberg LCL, Martin AM. Nonabelian geometric phase in the diamond nitrogen-vacancy center. Phys Rev A 2014;90:042116.
[51] Rashid M, Marko T, Ashley S, et al. Precession motion in levitated optomechanics. Phys Rev Lett 2018;121:253601.

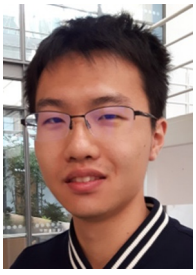

Xing-Yan Chen completed his B.Sc. degree in 2018 at Peking University. Then he had a two-month research internship at Tsinghua University, and now is a master student at Ludwig-Maximilians-Universität in München, and a researcher at Max-Planck-Institut für Quantenoptik, Germany. His research at Tsinghua University focused on quantum precision measurement and quantum information processing with solid spins. His current research interest is quantum simulation with ultracold polar molecules.

Zhang-Qi Yin is an Assistant Research Fellow at Center for Quantum Information, Institute for Interdisciplinary Information Sciences, Tsinghua University. From 1999 to 2009, he got his B.Sc., M.Sc., and Ph.D. degrees, all from Xi'an Jiaotong University, China. From 2007 to 2009, he was a visiting student in University of Michigan. From 2010 to 2012, he worked in Wuhan Institute of Physics and Mathematics, Chinese Academy of Sciences, and in University of Science and Technology of China. In 2012, he jointed Tsinghua University. His research interests include quantum information and optomechanics.